

NEW GUIDELINES



Production Editor, AICHE Journal
aicheproof@wiley.com

WILEY

PLEASE REFER TO THE JOURNAL ACRONYM AND ARTICLE NUMBER IN ALL CORRESPONDENCE. For example: **AICHE12345**

Dear Author,

Please correct your galley proofs carefully and return them within 24–48 hours to aicheproof@wiley.com.

This will be your only chance to review these proofs. Please note that the volume and page numbers shown on the proofs are for position only.

The editors reserve the right to publish your article without your corrections if they are not received in time.

Please annotate all corrections on the supplied PDF.

To avoid commonly occurring errors, please ensure that the following important items are correct in your proofs (Please note that once your article has been published online, no further corrections can be made):

Names of all authors present and spelled correctly (IMPORTANT: The addition or

deletion of author names in proofs is strictly prohibited and may result in the suspension or termination of your article's production.)

- Addresses and postcodes correct
- E-mail address of corresponding author correct and current
- Title of article correct
- All figures included and in the correct order
- All tables and equations correct (symbols and superscripts)
- All queries (included on the last page) answered

Note: the resolution of the figures in the PDF proofs is intentionally of lower quality to facilitate internet delivery. These images will appear at higher resolution and sharpness in the printed article.

Reprint Purchases: Should you wish to purchase additional copies of your article, please click on the link and follow instructions provided:

<https://caesar.sheridan.com/reprints/redirect.php?pub=10089&acro=AIC>

Please note that regardless of the form in which they are acquired, reprints should not be resold, nor further disseminated in electronic form, nor deployed in part or in whole in any marketing, promotional, or educational contexts without authorization from Wiley. Permissions requests should be directed to permissionsus@wiley.com

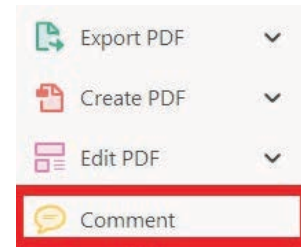
USING e-ANNOTATION TOOLS FOR ELECTRONIC PROOF CORRECTION

Required software to e-annotate PDFs: Adobe Acrobat Professional or Adobe Reader (version 11 or above). (Note that this document uses screenshots from Adobe Reader DC.)


The latest version of Acrobat Reader can be downloaded for free at: <http://get.adobe.com/reader/>

Once you have Acrobat Reader open on your computer, click on the [Comment](#) tab (right-hand panel or under the Tools menu).


This will open up a ribbon panel at the top of the document. Using a tool will place a comment in the right-hand panel. The tools you will use for annotating your proof are shown below:

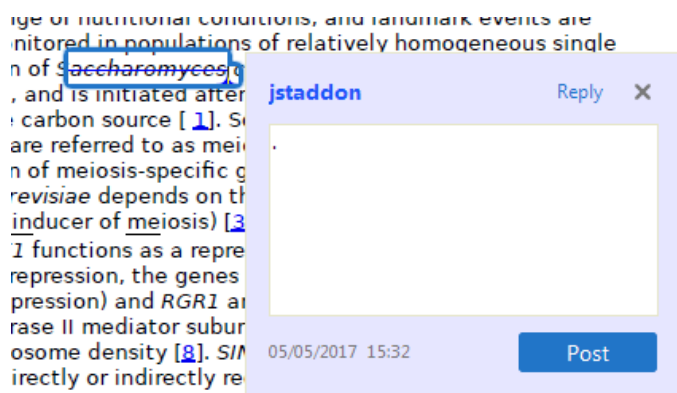


1. **Replace (Ins) Tool** – for replacing text.


 Strikes a line through text and opens up a text box where replacement text can be entered.

How to use it:

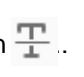
- Highlight a word or sentence.
- Click on .
- Type the replacement text into the blue box that appears.



2. **Strikethrough (Del) Tool** – for deleting text.

 Strikes a red line through text that is to be deleted.



How to use it:

- Highlight a word or sentence.
- Click on .
- The text will be struck out in red.


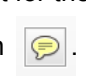
experimental data if available. For ORFs to be had to meet all of the following criteria:

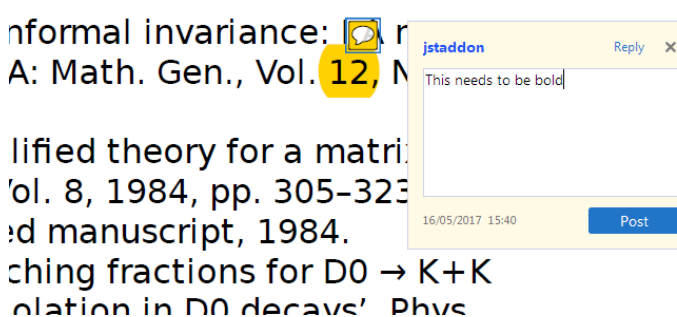
1. Small size (35-250 amino acids).
2. Absence of similarity to known proteins.
3. Absence of functional data which could not be the real overlapping gene.
4. Greater than 25% overlap at the N-terminus terminus with another coding feature; over both ends; or ORF containing a tRNA.

3. **Commenting Tool** – for highlighting a section to be changed to bold or italic or for general comments.


  Use these 2 tools to highlight the text where a comment is then made.

How to use it:


- Click on .
- Click and drag over the text you need to highlight for the comment you will add.
- Click on .
- Click close to the text you just highlighted.
- Type any instructions regarding the text to be altered into the box that appears.

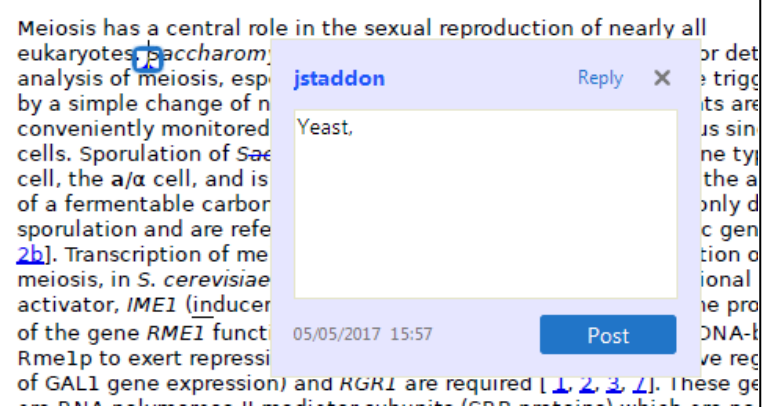


4. **Insert Tool** – for inserting missing text at specific points in the text.


 Marks an insertion point in the text and opens up a text box where comments can be entered.

How to use it:


- Click on .
- Click at the point in the proof where the comment should be inserted.
- Type the comment into the box that appears.



5. Attach File Tool – for inserting large amounts of text or replacement figures.

 Inserts an icon linking to the attached file in the appropriate place in the text.


How to use it:

- Click on .
- Click on the proof to where you'd like the attached file to be linked.
- Select the file to be attached from your computer or network.
- Select the colour and type of icon that will appear in the proof. Click OK.


The attachment appears in the right-hand panel.

chondrial preparator
ative damage injury
re extent of membra
i, malondialdehyde (TBARS) formation.
used by high perform

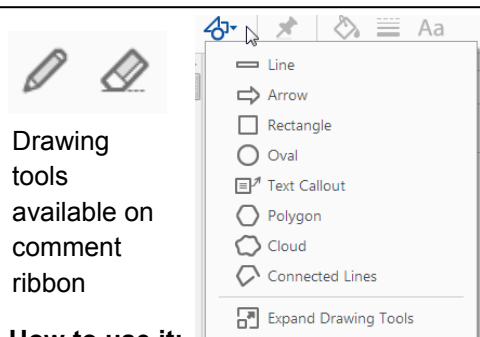
6. Add stamp Tool – for approving a proof if no corrections are required.

 Inserts a selected stamp onto an appropriate place in the proof.

How to use it:

- Click on .
- Select the stamp you want to use. (The **Approved** stamp is usually available directly in the menu that appears. Others are shown under *Dynamic*, *Sign Here*, *Standard Business*).
- Fill in any details and then click on the proof where you'd like the stamp to appear. (Where a proof is to be approved as it is, this would normally be on the first page).

of the business cycle, starting with the
on perfect competition, constant ret
production. In this environment goods
extra costs should be set to zero for the
he market. The New-Keynesian model is
etermined by the model. The New-Keynesian
otaki (1987), has introduced produc
general equilibrium models with nomin
and downward sloping demand curves. Most of this literature

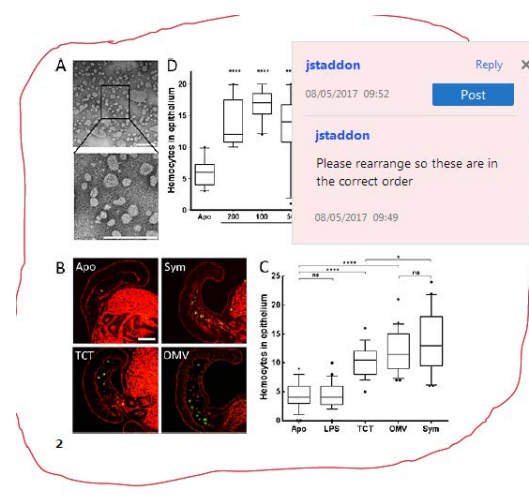


7. Drawing Markups Tools – for drawing shapes, lines, and freeform annotations on proofs and commenting on these marks.

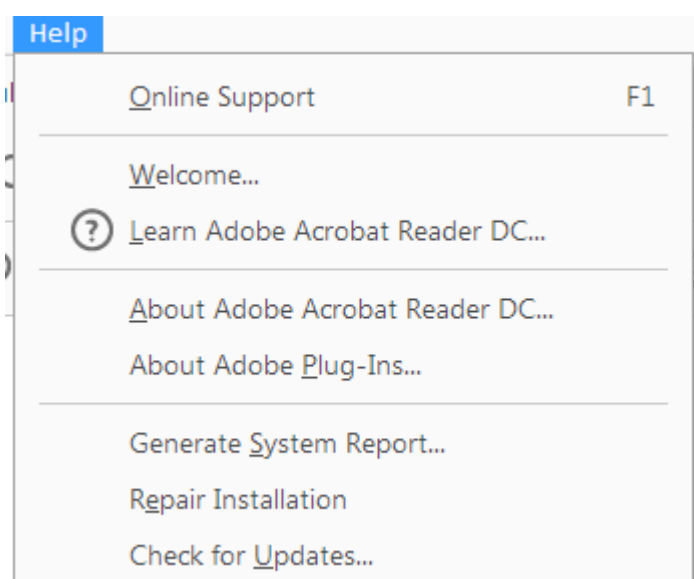
Allows shapes, lines, and freeform annotations to be drawn on proofs and for comments to be made on these marks.

How to use it:

- Click on one of the shapes in the **Drawing Markups** section.
- Click on the proof at the relevant point and draw the selected shape with the cursor.
- To add a comment to the drawn shape, right-click on shape and select *Open Pop-up Note*.
- Type any text in the red box that appears.



For further information on how to annotate proofs, click on the **Help** menu to reveal a list of further options:



WILEY

COLOR REPRODUCTION IN YOUR ARTICLE

Color figures were included with the final manuscript files that we received for your article. Because of the high cost of color printing, we can only print figures in color if authors cover the expense. **The charge for printing figures in color is \$700 per figure.**

Please indicate if you would like your figures to be printed in color or black and white. Color images will be reproduced online in *Wiley Online Library* at no charge, whether or not you opt for color printing.

Failure to return this form will result in the publication of your figures in black and white.

JOURNAL _____ VOLUME _____ ISSUE _____

TITLE OF MANUSCRIPT _____

MS. NO. _____ NO. OF COLOR PAGES _____ AUTHOR(S) _____

Please print my figures in black and white

Please print my figures in color

\$ _____

Purchase

BILL TO:

Name _____ **Order No.** _____

Institution _____ Phone _____

Address _____ Fax _____

_____ E-mail _____

Author Query Form

Journal: AIC

Article: 15990

Dear Author,

During the copyediting of your manuscript the following queries arose.

Please refer to the query reference callout numbers in the page proofs and respond to each by marking the necessary comments using the PDF annotation tools.

Please remember illegible or unclear comments and corrections may delay publication.

Many thanks for your assistance.

Query References	Query	Remarks?
AQ1	AUTHOR: Please check whether edit made in the title is OK as typeset.	OK AQ10: OK
AQ2	AUTHOR: Please check whether affiliations are OK as typeset.	OK
AQ3	AUTHOR: Please confirm that the corresponding author information is OK as typeset.	OK
AQ4	AUTHOR: Please check whether reference in abstract is OK as typeset.	OK
AQ5	AUTHOR: Please note that Ref. 9 is set as Ref. 4 as it seems to be the same as the latter. Hence renumbering has been done. Please check.	revised and corrected
AQ6	AUTHOR: Please note that "Supporting Information" is cited in text but not provided in the manuscript. Please check.	File added
AQ7	AUTHOR: Please provide author details for Ref. 31 and also confirm whether Ref. 31 is OK as typeset.	OK
AQ8	AUTHOR: Please confirm whether figure legends are OK as typeset.	revised and corrected
AQ9	AUTHOR: Please check whether table captions and table footnotes of all Tables are OK as typeset.	revised and corrected
AQ10	AUTHOR: Please confirm that given names (red) and surnames/family names (green) have been identified correctly.	Are OK

Funding Info Query Form

Please confirm that the funding sponsor list below was correctly extracted from your article: that it includes all funders and that the text has been matched to the correct FundRef Registry organization names. If a name was not found in the FundRef registry, it may be not the canonical name form or it may be a program name rather than an organization name, or it may be an organization not yet included in FundRef Registry. If you know of another name form or a parent organization name for a "not found" item on this list below, please share that information.

FundRef name	FundRef Organization Name
Consejo Nacional de Investigaciones Científicas y Técnicas (CONICET), Agencia Nacional de Promoción Científica y Tecnológica (ANPCyT) of Argentina	Consejo Nacional de Investigaciones Científicas y Técnicas
Facultad de Ingeniería Química, Universidad Nacional del Litoral (UNL)	[NOT FOUND IN FUNDREF REGISTRY]
Universidad Nacional del Litoral	Universidad Nacional del Litoral

UNL means Universidad Nacional del Litoral

Facultad de Ingeniería Química is a faculty (collage) belonging to the Universidad Nacional del Litoral

WILEY
Author Proof

Model Based Analysis of Lithium Batteries Considering Particle-Size Distribution

E. R. Henquín  and P. A. Aguirre

Instituto de desarrollo y diseño (INGAR), Consejo Nacional de Investigaciones Científicas y Técnicas (CONICET), Avellaneda 3657, Santa Fe S3002GJC, Argentina

Facultad de Ingeniería Química, Universidad Nacional del Litoral, Santiago del Estero 2829, Santa Fe S3000AOM, Argentina

DOI 10.1002/aic.15990

Published online in Wiley Online Library (wileyonlinelibrary.com)

Performance of lithium ion batteries whose electrodes are composed of particles of different sizes is studied. Simplified model developed in (Henquín and Aguirre, AICHE J. 2015; 61:90–102) is extended and the simulations are compared with experiments from the literature so as to validate this new model. The differences in current density observed in particles of different sizes, which are in contact, depend on particle size and state of charge. Internal particle to particle discharge currents are observed during relaxation times. A parametric study of the applied current and particle sizes of electrodes is performed to evaluate cell performance, with emphasis on cell voltage and final capacity measurement. The evolution of reaction rates on the surface of electrode particles and their corresponding states of charge are depicted. An analysis of relaxation times in terms of cell voltage, current density, equilibrium potentials, and overpotentials is included. © 2017 American Institute of Chemical Engineers AICHE J, 00: 000–000, 2017

Keywords: lithium ion batteries, different particle size, simplified mathematical modeling

Introduction

High power lithium batteries manufacturing and use for mobile applications (such as cars), or stationary (energy storage in homes and public buildings) have become very promising due to their multiple advantages.¹ The market of high energy density and power storage batteries is constantly expanding.² However, for the proper operation of these units, a very thorough control of the variables involved in charge and discharge processes must be taken. Therefore, it is necessary to count on phenomenological and predictive mathematical models (rigorous but simple to interpret and solve) that are capable of predicting the phenomena produced in batteries. Thus, Doyle et al.³ developed a novel theoretical model for uniform particle size batteries which was corroborated by experimental points at charge and discharge of two different batteries. However the predictive capacity of this model strongly depends on ad hoc parameters to achieve the adjustments with experimental results, as recognized by the authors themselves, as they frequently have to resort to correlative parameters to achieve the adjustments with experimental data points. The model also has several coupled Partial Differential Algebraic Equations to be resolved. Thus, with the aim of facilitating resolution and reducing calculation times,

a series of model reformulations³ are presented in Ref. 4. Other authors have worked on simplified mathematical models that are analogous to electric circuits,^{5,6} thus obtaining very fast models involving lesser phenomenological predictive capacity compared to the previously mentioned. In a previous paper,⁷ we presented a simplified mathematical model, based on mass and energy balance equations. The main advantages of our model compared with other models mentioned above are that (i) currents balances are used correctly and properly (Eq. 6), which are integral equations instead as local one as is the case in the original work³ (ii) a theoretical based equation for the conductivity of electrolyte (Eq. 10) is used, with better adjustments to the experimental points compared to the original work, as shown in Figure 2 (iii) the model results in a set of ordinary differential and algebraic equations, very simple to solve (iv) no parametric adjustments as contact resistance are necessary (v) the model can be reduced to a simpler entirely algebraic system, which also fits with the experimental points. In summary the model is highly predictive and simple enough to be solved even in spreadsheet calculations.

To achieve simple mathematical models and rapid resolution, some authors sacrifice predictive power, despising certain phenomena or including strong simplifications. In facilities where the use of large banks of lithium batteries is required, it is not convenient to take extreme simplifications in mathematical models because high-capacity batteries are used in cycles and are subjected to different charge and discharge rates. In this sense, many authors have shown a growing interest in developing mathematical models, focusing their attention on

Additional Supporting Information may be found in the online version of this article.

Correspondence concerning this article should be addressed to E. R. Henquín at chenquin@santafe-conicet.gov.ar.

© 2017 American Institute of Chemical Engineers

77 the phenomena produced in electrode particles. Thus, in Ref.
 78 9, a model considering a single particle is developed by Zhang
 79 et al. The results of three models of different complexities are
 AQ5 80 compared in Ref. 4. An early work describing a pseudo 2D
 81 model that includes diffusion inside particles, diffusion in
 82 electrolyte phase, and that incorporates Butler-Volmer kinetics
 83 was performed by Doyle et al.¹⁰

84 The need for mathematical models to predict the phenom-
 85 ena occurring inside batteries becomes evident, taking into
 86 account particle-size distribution on electrodes. An extensive
 87 review of mathematical models considering the number of
 88 particles in electrodes was performed in Ref. 11. Experimen-
 89 tal work with X-ray studying the effect of electrode micro-
 90 structure of batteries was performed in Ref. 12. In Ref. 13,
 91 the amount of Li⁺ ion intercalated in natural carbon flakes
 92 whose particle size ranges from 2 to 40 μm was experimen-
 93 tally studied. In others studies,^{14–23} the close relationship
 94 between particle size and electrode morphology, among
 95 other variables, was confirmed for battery performance. In
 96 Ref. 14, the improvement of the electrochemical properties
 97 of particles by decreasing particle size was suggested. A
 98 mathematical model describing the effect of electrode micro-
 99 structure on galvanostatic discharge was performed in Ref.
 100 17. The finite element method was used, and solid-
 101 electrolyte interface potential, equilibrium potential, and
 102 ohmic drop were related. In Ref. 21, self-discharge rate is
 103 related to electrode particle size and electrode surface area.
 104 The authors of Ref. 22 focus their attention on conductive
 105 additives and the distinction between primary particle,
 106 aggregate, and agglomerate.

107 **Conversely**, the performance of large storage systems can
 108 be affected by the use of an improper technique for selecting
 109 particle size. Thus, in Ref. 23 the effect of particle size and
 110 electrode thickness on the reaction rate is studied. A mathe-
 111 matical model and experiments are presented by the authors of
 112 Ref. 24. They use an empirical expression that takes into
 113 account the number of contacts between solid particles and the
 114 average contact resistance. In addition to calculating transport
 115 properties, a discretization of the actual particle-size distribu-
 116 tion is used

117 In Ref. 25, the effect of particle size and speed of cycling,
 118 among other variables, on the specific energy of batteries is
 119 theoretically addressed. This issue has attracted the attention
 120 of authors who attempted to study the consequences of this
 121 problem in large units. So, Kenney et al.²⁶ extended the single
 122 particle model to study a system of batteries—used to supply
 123 power for a home—which had slight variations in electrode
 124 manufacturing. In Ref. 27, the problem of coexistence of dif-
 125 ferent particle sizes is also shown. Darling and Newman
 126 developed a mathematical model based on,¹⁰ which was
 127 applied to a cell whose positive electrode is Li_yMn₂O₄, and its
 128 negative is a lithium foil. The work studies the influence of
 129 considering two different particle sizes on the states of charge
 130 in cycles, temporary cell voltage responses, and relaxation
 131 times. Unfortunately, and as it was mentioned in Ref. 7, these
 132 models have multiple differential equations coupled with their
 133 contour conditions.

134 Lithium Iron-Phosphate batteries are studied in Ref. 28,
 135 emphasizing the existence of diffusion areas in the solid phase.
 136 In the same way, the authors propose the model with two-size
 137 electrode particles, but considering the same surface area and
 138 volume fraction as those of a single-size particle battery. The
 139 authors of Ref. 29 emphasize the idea of diffusion directions

in the solid phase and the idea of incorporating a distribution
 of particle sizes to describe battery behavior.

Based on the study of these bibliographies, it is demon-
 strated the importance of simplified mathematical modeling,
 and the interest in studying the impact of particle-size distribu-
 tion in the electrodes on the performance of the battery.
 Hence, in this article, the mathematical model presented in
 Ref. 7 is extended and adapted to calculate cell voltage, reac-
 tion rates, states of charge, equilibrium potentials, and other
 ohmic drops inside the battery, considering that electrodes are
 composed by particles of two different sizes. The model is val-
 idated by comparing theoretical predictions with experimental
 points of two batteries using different electrode materials. A
 parametric study of battery variables is performed with the
 aim of studying the temporal response to different discharge
 conditions and considering different particle sizes. Internal
 currents inside the battery along relaxation processes are
 computed.

Theoretical Considerations

As previously stated, the mathematical model being used
 has its bases published in Ref. 7 and is adjusted to a system
 of more than one particle. Thus, the salt balance in the elec-
 trolyte is

$$\frac{dC_e^A}{dt} = \sum_m j_m^A (1 - t_+^o) \frac{a_{e/s,m}^A}{v_e^A} n_m - K_1^A (C_e^A - C_e^S) \frac{a_{tr,e}^A}{v_e^A} \quad (1)$$

$$\frac{dC_e^C}{dt} = \sum_m -j_m^C (1 - t_+^o) \frac{a_{e/s,m}^C}{v_e^C} n_m + K_1^C (C_e^S - C_e^C) \frac{a_{tr,e}^C}{v_e^C} \quad (2)$$

$$\frac{dC_e^S}{dt} = K_1^A (C_e^A - C_e^S) \frac{a_{tr,e}^A}{v_e^S} - K_1^C (C_e^S - C_e^C) \frac{a_{tr,e}^C}{v_e^S} \quad (3)$$

where K_1^A and K_1^C can be considered as a global mass-transfer
 coefficient between anode and separator and separator and
 cathode; and it can be calculated as

$$\frac{1}{K_1^i} = \frac{L^i/2}{D_{eff}^i} + \frac{L^S/2}{D_{eff}^S} \left(\frac{\epsilon_1^i + \epsilon_p^i}{\epsilon_1^S + \epsilon_p^S} \right) \quad (4)$$

where, by convention, i will be anode or cathode, in that order;
 and m refers to particle size. It is important to emphasize that
 this coefficient arises from the previous manipulation of the
 written equations and is not a definition coming from a simpli-
 fication. **Conversely**,

$$D_{eff}^i = D_{e,o} \left(\epsilon_1^i + \epsilon_p^i \right)^{\gamma_{D,i}} \quad (5)$$

is the effective coefficient of electrolyte phase diffusion.

It is noteworthy that summations in Eqs. 1 and 2 are
 extended for m particles.

The heretofore defined equations involve the volume frac-
 tion of phase j in compartment i: ϵ_j^i is defined in the same
 way as reported in Ref. 7. In this work, however, a study
 where batteries are made up of different particle sizes is per-
 formed. Consequently, it is necessary to redefine the frac-
 tions of the different phases that constitute the electrodes.
 These definitions are explained below in the 'Multiparticle
 Model' section.

182 The contact area between spherical particles and electrolyte
183 phase, and the volume of different phases are expressed by

$$a_{e/s,m}^i = 4\pi R_{s,m}^i{}^2 \quad (6)$$

$$a_{tr,e}^i = a_t (\epsilon_1^i + \epsilon_p^i) \quad (7)$$

$$v_e^i = a_t L^i (\epsilon_1^i + \epsilon_p^i) \quad (8)$$

$$v_s^i = a_t L^i \epsilon_s^i \quad (9)$$

184 Following this line of work Ref. 7, where particles are discre-
185 tized into three parts (internal, external, and surface), mass
186 balance on electrode particles is

$$v_{m,s,int}^j \frac{dC_{m,s,int}^i}{dt} = \mp D_{ms}^i \frac{(C_{m,s,int}^i - C_{m,s,ext}^i)}{(\delta_{m,2}^i + \delta_{m,3}^i)} a_{m,int}^i \quad (10)$$

$$v_{m,s,ext}^j \frac{dC_{m,s,ext}^i}{dt} = \pm D_{ms}^i \frac{(C_{m,s,int}^i - C_{m,s,ext}^i)}{(\delta_{m,2}^i + \delta_{m,3}^i)} a_{m,int}^i \mp j_m^i a_{m,ext}^i \quad (11)$$

$$C_{m,surf}^i(t) = C_{m,s,ext}^i(t) \mp j_m^i \frac{\delta_{m,4}^i}{D_{ms}^i} \quad (12)$$

187 where signs are consistent with the order of i. It is worth men-
188 tioning that $\delta_{m,j}^i$ are diffusion distances inside the particles,
189 and their calculation may be consulted in Ref. 7 (Figure 4).

190 As can be seen, manipulation of the above equations has
191 resulted in a mathematical model that should not be assumed to
192 be a simplification of a p2d or similar models, but rather a new
193 model arising entirely from an integral mass balance (in space)
194 and differential in time of averaged properties. In this way, the
195 set of equations that represent the evolution of concentrations
196 (both in the compartments and in the particles), are equations
197 that retain the character of differential in the field of time, but
198 are integral equations in the space coordinates (both in the
199 thickness of the electrodes as in the radius of the particles).

200 Simplified diagram concentration profiles of both electro-
201 lyte and particle phase can be seen in Ref. 7, Figures 3, and 4.

202 Conduction electrolyte properties are evaluated with the
203 simplified expression A-2 of Ref. 3, used in Ref. 7 (Eq. 8)

$$\Delta\phi_e^A = -\frac{j_e^A L^A}{\kappa_{eff}^A} + \frac{RgT}{F} (1 - t_+^o) 2 \frac{(C_e^A - C_e^{A,S})}{C_e^A} \quad (13)$$

204 being

$$\kappa_{eff}^i = \kappa_o^i (\epsilon_1^i + \epsilon_p^i)^{\gamma_{\kappa,i}} \quad (14)$$

205 the effective conductivity of electrolyte phase, and

$$\kappa_o^i = \left[\frac{(1 + K0 C_e^i)^2}{(1 - K1 C_e^i)^2 + (1 + K2 C_e^i)^2 + K3} \right] \frac{1}{K4} \quad (15)$$

206 is conductivity of the salt solution. The parameters of Eq. 15
207 can be consulted in Table 2 of Ref. 7. This approach is pre-
208 ferred rather than the typical polynomial presented in Ref. 3 as
209 it presents only one maximum conductivity value at normal
210 working concentrations.

211 The potential drop in solid phase can be expressed as

$$\Delta\phi_{ms}^i = i_{ms}^i L^i / \sigma_{eff}^i \quad (16)$$

where effective conductivity σ_{eff}^i is expressed as

$$\sigma_{eff}^i = \sigma_o^i (\epsilon_s^i + \epsilon_f^i)^{\gamma_{\sigma,i}} \quad (17)$$

Overpotentials are calculated by the Butler-Volmer equation

$$\eta_m^i = \frac{RgT}{0.5F} \sinh^{-1} \left(\frac{j_m^i F}{2 j_0^i} \right), \text{ with} \quad (18)$$

$$j_0^i = k^i [C_{m,surf}^i C_e^i (C_{m,max}^i - C_{m,surf}^i)]^{0.5}$$

and the total applied current, similarly to that shown in Ref. 7,
is calculated by

$$i_{app} = F 4 \pi \sum_m j_m^i n_m^i R_{s,m}^i{}^2 \quad (19)$$

As it will be seen later, it should be noted that, if the battery
is composed of particles of a single radius, the fraction of the
current drained by particles is equal to 1. However, if batter-
ies have electrode particles of different sizes, fraction is a
value between 0 and 1 for each different particle. Also, if the
battery being studied is at a stage of charge, relaxation, or
discharge, this fraction of current changes over time. Thus, it
is defined as

$$\text{fraction}_m^i = j_m^i F 4 \pi n_m^i R_{s,m}^i{}^2 / i_{app} \quad (20)$$

Conversely, open circuit potentials vs. state of charge on both
electrodes are represented by the functionality

$$\theta_m^i = C_{surf,m}^i / C_{max,m}^i \quad (21)$$

As in this study we will compare the results of our models
against experimental data about batteries made of different
electrode materials which were extracted from works by other
authors, the equations used to represent the equilibrium poten-
tials of different batteries are listed in the Appendix (Support-
ing Information).

Multiparticle model

In the first part of this work, the relationship between the
numbers of particles is fixed

$$n_m^i / n_n^i \quad (22)$$

where i represents anode or cathode; and m and n identifies
particle size.

In case of only two different particle sizes, namely "size 1"
and "size 2," the following relations are used

$$\epsilon_{s,m}^i = \frac{\epsilon_s^i}{(R_{s,n}^i / R_{s,m}^i)^3 n_m^i / n_n^i + 1} \quad (23)$$

$$\epsilon_{s,n}^i = \epsilon_s^i (R_{s,n}^i / R_{s,m}^i)^3 n_m^i / n_n^i \quad (24)$$

and finally the number of each particle in electrodes is

$$n_n^i = \epsilon_{s,n}^i a_t L^i / (4/3 \pi R_{s,n}^i{}^3) \quad (25)$$

Electrolyte phase and solid phase currents are calculated as in
Ref. 7, where

$$i_e^i = \frac{i_{app}/2}{(\epsilon_1^i + \epsilon_p^i)} \quad (26)$$

Table 1. Adjustable Design Parameters Corresponding to Battery 1: $\text{Li}_x\text{C}_6|\text{Li}_y\text{Mn}_2\text{O}_4$

Parameter	Anode Li_xC_6	Cathode $\text{Li}_y\text{Mn}_2\text{O}_4$	Separator
ϵ_1	0.357	0.444	0.724
ϵ_p	0.146	0.186	0.276
ϵ_f	0.026	0.073	
L (cm)	0.01	0.0174	0.0052
γ_κ	3	3	
D_s ($\text{cm}^2 \text{s}^{-1}$)	3.9×10^{-10}	1.0×10^{-9}	
σ_0 (S cm^{-1})	1.0	0.038	
k ($\text{A cm}^{1/2} \text{mol}^{-1/2}$)	0.18793	0.20803	
R_s (cm)	Particle 1	0.0013125	0.0008925
	Particle 2	0.001	0.00068
γ_σ	1	1.5	
γ_D	3	3	
C_s^{max} (mol cm^{-3})	0.02639	0.02286	
C_s^0 (mol cm^{-3})	0.01487	0.0039	
C_e^0 (mol cm^{-3})		0.002	
D_e ($\text{cm}^2 \text{s}^{-1}$)		1.51×10^{-6}	
Ntpte		0.363	

$$i_{s,n}^i = \frac{i_{\text{app}}/2}{\left(n_n^i \pi R_{s,n}^i + n_m^i \pi R_{s,m}^i \right)} \quad (27)$$

243 As it was discussed in Ref. 7, current density of electrolyte
244 phase in the separator is expressed as

$$i_e^S = i_{\text{app}} a_t / a_{\text{tr,e}}^S \quad (28)$$

245 Taking into account the definition of overpotential and consid-
246 ering continuity of the electric field for particle “1” in contact
247 with particle “2,” then

$$U_{\theta,1}^i \pm \eta_1^i = U_{\theta,2}^i \pm \eta_2^i \quad (29)$$

248 where (\pm) is function of the anode (+) or cathode (-).

249 Finally, the cell potential, considering that the battery con-
250 sists of two-size particles, is calculated by

$$U_{\text{cell}} = \left(U_{\theta,1 \text{ or } 2}^C - \eta_{1 \text{ or } 2}^C \right) - \left(U_{\theta,1 \text{ or } 2}^A + \eta_{1 \text{ or } 2}^A \right) - \Delta\phi_s^C - \Delta\phi_s^A - \Delta\phi_c^C - \Delta\phi_c^A - \Delta\phi_e^S \quad (30)$$

251 Resolution of the Equations System

252 Batteries considered in this article have insertion electrodes
253 whose particles can have different sizes. The general idea of
254 resolution was developed considering that the batteries have
255 only two particle sizes, but the same analysis can be easily
256 extended to three or more different particle sizes. Likewise to
257 Ref. 7, the calculation scheme was developed by setting con-
258 stant current value and calculating cell potential over time.
259 However, this scheme can be easily adapted for calculations in
260 other conditions, for example, constant discharge power.

261 The calculus scheme was implemented in different program-
262 ming environments to reduce errors. Gams,³⁰ was used to solve
263 the system of equations simultaneously. A sequential and itera-
264 tive calculation was implemented in SciLab.³¹ Calculation
265 times varied depending on the simulated current. For smaller
266 currents (discharge times of about 40,000 s), normal computa-
267 tion times using the sequential scheme were 300 s. For higher
268 currents, calculation times in discharge were 2 s on average.
269 However, when the battery is in relaxation mode, calculation
270 times were increased by 200 s. When the system was solved
271 simultaneously with Gams, the calculation time was 2 s.

Validation and Comparison with Experimental Data

272 For comparison with the experimental points, the developed
273 model is used considering particles of two different sizes in
274 each electrode. To achieve the results that best fit the experi-
275 mental points, the following procedure was applied: one parti-
276 cle was left in its original size (reported in the corresponding
277 paper), and the other particle size was varied. In some cases it
278 was necessary to vary both particle sizes, with respect to its
279 original size. In each of the cases treated, the corresponding
280 details are reported.

281 This methodology can be extended to a distribution of parti-
282 cle sizes.
283
284

Battery 1: $\text{Li}_x\text{C}_6|\text{Li}_y\text{Mn}_2\text{O}_4$

285 In Ref. 7, the comparison with experimental data (Doyle
286 et al.³) for two different cell types was presented, using a
287 model that considers only a single particle size.
288

289 The experimental points were collected by the authors of
290 Ref. 3 by performing constant current discharges. The two bat-
291 teries used by the authors, differed mainly in the thickness of
292 the electrodes, and the type of electrolyte used. Also in the
293 original work, charging experiments were performed. How-
294 ever, they were not taken into account in our work.⁷ In this
295 article, we choose for our simulations, battery called as Cell 1
296 by the authors of.³ Table 1 shows the physical parameters and
297 the physicochemical properties representative for this battery.
298 In addition, as we explain below, the particle sizes used in our
299 simulations are detailed.

300 The particular focus of this section is to improve the quality
301 of the comparison that we made in Ref. 7, considering this
302 model, which takes into account two different particle sizes.

303 In all simulations performed with this model considering
304 two particles sizes, the same amount of active material and the
305 same fraction of solids in each electrode were fixed. Also the
306 number of small particles was set equal to the number of large
307 particles.

308 Comparisons with experimental results of battery discharge
309 were slightly improved compared to the results presented in
310 Ref. 7. To do that, a parametric sensitivity analysis was per-
311 formed by varying the particle sizes in the simulations to
312 achieve the best results. The chosen strategy was increasing

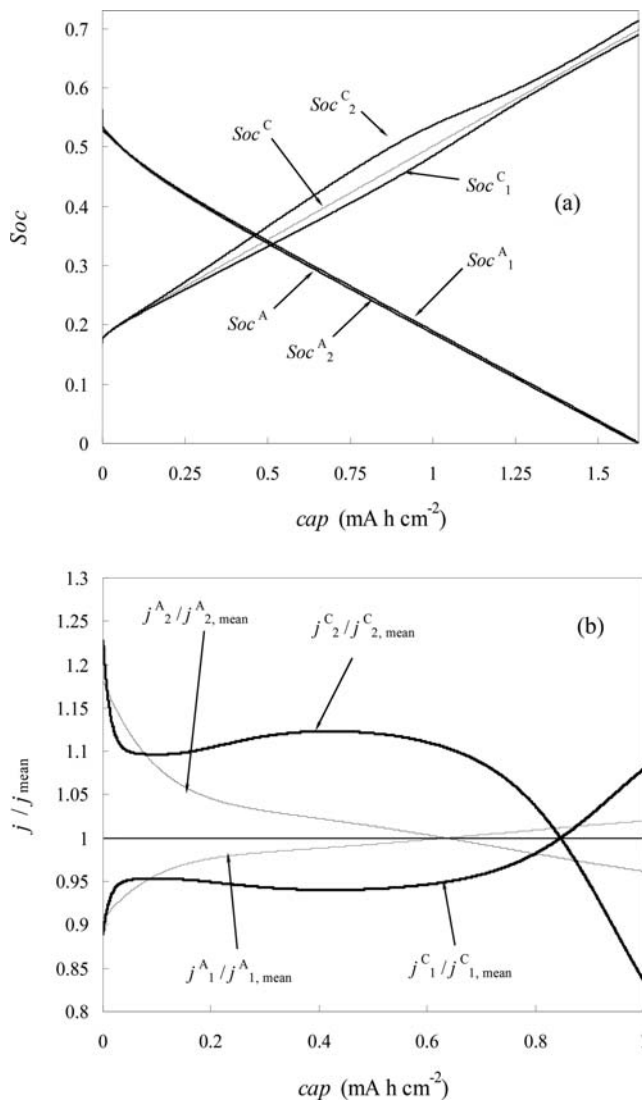


Figure 1. Comparison of results considering one and two particle sizes. Battery 1: $\text{Li}_x\text{C}_6|\text{Li}_y\text{Mn}_2\text{O}_4$. Particle 1: increased 5% and particle 2: decreased 20% from the original size (a) States of charge. $i_{\text{app}} = 0.0035 \text{ Acm}^{-2}$ (b) Dimensionless electrochemical reaction rate. $i_{\text{app}} = 0.007 \text{ Acm}^{-2}$.

313 5% of the original size of the particle called “1,” and reducing
 314 by 20% the size of the particle called “2,” from its original
 315 size. These comparisons are not shown in this article as they
 F6 316 are very similar to those shown in Ref. 7 (Figure 6a). How-
 317 ever, the behavior of others physicochemical variables of these
 318 batteries can be analyzed, considering these two different par-
 F1 319 ticles sizes. Thus, in Figure 1a, the results of the evolution
 320 of the states of charge ($\text{Soc}_{1\text{or}2}^{\text{C}}$) for a given discharge current of
 321 anodic and cathodic particles compared to those produced con-
 322 sidering a single particle size (Soc^{C}) are shown. Current den-
 323 sities and states of charge in cathodic particles are clearly
 324 affected by the particle-size distribution. However, the average
 325 value of the states of charge approaches the value of state of
 326 charge of the battery considering a single particle size. Also,
 327 in Figure 1b, the evolutions of dimensionless reaction rates
 328 are displayed. These evolutions are affected significantly when
 329 different particle sizes are considered. At the beginning of

discharge, reaction rates change significantly, ranging from 330
 5% to 12% in a short time. Then the battery begins a period of 331
 relatively little change in reaction rates, and the discharge is 332
 controlled by ohmic losses. Finally, in the last stage of dis- 333
 charge, a zone of great change in the variables is noticed. 334
 These variations are most apparent for cathode particles and 335
 are associated with shape potential equilibrium curve, as dis- 336
 cussed below. 337

Battery 2: $\text{Li}_x\text{C}_6|\text{Li}_y\text{CoO}_2$ 338

Experimental data of this kind of battery were extracted from 339
 Ref. 8. The authors of this paper have used a Sony battery 340
 18,650 With 1.8 Ah rated capacity. Experiments were conducted 341
 similar to the case described above. The battery was charged to 342
 an approximate voltage of 4.2 volts, and then it was discharged 343
 at constant current conditions, to voltages near 2 volts. 344

In this article, the evolution of the performance of the bat- 345
 tery with the number of cycles (N) at two different tempera- 346
 tures was experimentally studied. In addition the authors 347
 developed a mathematical model to fit the experimental points, 348
 proposing semiempirical equations, which describe: the 349
 change in state of charge, the change of film resistance, and 350
 the change of the solid phase diffusion coefficient, as a func- 351
 tion of number of cycles, for two different temperatures. 352

All parameters used to simulate this battery, were adopted 353
 from Ref. 8, except: 354

- i. A model of the separator, which has the same potential 355
 drop as the one informed in the original work. 356
- ii. The initial state of charges. For anodic particles is 357
 0.838 and for cathodic particles is 0.375. 358

For comparison with experimental points of battery dis- 359
 charge, the following strategy was selected: particles “2” are 360
 larger than particles “1”; in the anode particle “2” is 80% 361
 larger than the particle “1,” and in the cathode particle “2” is 362
 20% larger than the particle “1.” Sizes of particle “1” was set 363
 to the same value as in the original paper. These values, and 364
 all the parameters used in the simulations for this battery, are 365
 reported in Table 2. 366 T2

The three empirical equations described in the original 367
 paper (state of charge, particle diffusivity, and resistance) are 368
 not used in our model. Instead, we simulated performance 369
 loss, by decreasing the amount of particles as function on the 370
 number of cycles. 371

Physically this loss of performance may be due to, electrical 372
 contacts between some particles no longer exists, or due to the 373
 formation of an extra resistance on the surfaces of the partic- 374
 les. This issue was widely discussed in the literature (e.g.³). 375

In our simulations, the number of particles “2” both in 376
 anode and cathode diminishes as function of number of cycles. 377
 Figures 2a, c shows the agreement between the experimental 378 F2
 points and the results of our model, at 25 and 50°C, respec- 379
 tively. The larger particles in both anode and cathode, 380
 decreases according to number of cycle, as it is shown in Fig- 381
 ures 2b, 2d, for 25 and 50°C. 382

Therefore, in these simulations the total amount of active 383
 material of the cell decreases as the number of cycles 384
 increases. We assume that the active material lost, corresponds 385
 to particles that lose electrical contact with neighbors 386
 particles. 387

Parametric Study using Two Particle Sizes 388

A parametric study is performance to identify the model 389
 response under different discharge conditions. The simulated 390

Table 2. Adjustable Design Parameters Corresponding to Battery 2: $\text{Li}_x\text{C}_6|\text{Li}_y\text{CoO}_2$

Parameter	Anode Li_xC_6	Cathode Li_yCoO_2	Separator
ϵ_1	0.485	0.385	1
L (cm)	0.0088	0.008	0.008
D_s ($\text{cm}^2 \text{s}^{-1}$)	3.9×10^{-10}	1.0×10^{-9}	
σ_{eff} (S cm^{-1})	0.005766	0.1211	
k ($\text{A cm}^{5/2} \text{mol}^{-3/2}$)	0.2045	0.0981	
R_s (cm)	Particle 1 Particle 2	0.0020 0.0024	
C^{max} (mol cm^{-3})		0.051555	
C_0^b (mol cm^{-3})	0.030555	0.01933 ^b	
C_0^c (mol cm^{-3})	0.02563 ^a	0.001	
D_e ($\text{cm}^2 \text{s}^{-1}$)		7.5×10^{-6}	
Area (m^2)		0.0796	
ntpte		0.363	

AQ9

^aBased on Data of Table 1⁸; $\theta_{\text{initial}}^A = 0.838$.
^bAdopted from Table 1⁸; $\theta_{\text{initial}}^C = 0.375$.

391 battery, in this section, (considering only one particle size) is
 392 detailed in Ref. 7, identified as cell A, and is the same battery
 393 mentioned in the 4th section. In each section discussed below,
 394 we detail the parameters changed, and the conditions these
 395 changes were made.
 396 In this article we consider that each electrode contains par-
 397 ticles of two different sizes: Particles of size “1” called par-
 398 ticles “1” and particles of size “2” called particles “2.”
 399 The methodology used in this study consists of setting particle
 400 size “1” for both anodic and cathodic electrodes, in its original

size (shown in Table 1, according with the experiments and sim- 401
 402 ulation of the original paper), and varying particle size “2.” The
 403 total amount of solid material is maintained constant in both
 404 anode and cathode. This condition is imposed from the above
 405 Eqs. 22–29, in which the total solid fraction remains constant in
 406 each electrode. Furthermore, the number of particles “1” is set
 407 equal to the number of particles “2.” As a consequence, the total
 408 number of particles diminishes as the size of particles “2”
 409 increases. According to these constraints, all following compar- 410
 411 isons involve batteries with the same amount of active material.

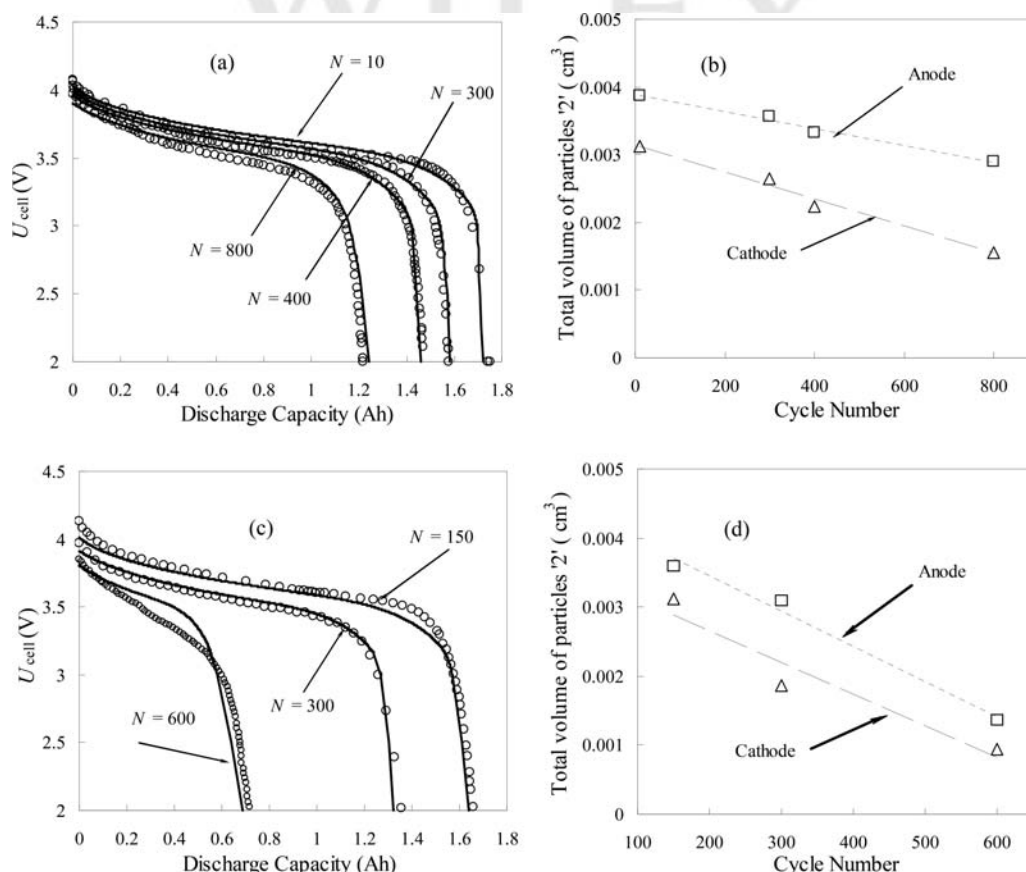


Figure 2. Comparison between experimental points⁸ and the model developed in this article Battery 2: $\text{Li}_x\text{C}_6|\text{Li}_y\text{CoO}_2$.

(a) and (b) $T = 25^\circ\text{C}$. (c) and (d) $T = 50^\circ\text{C}$ Left: Cell potential. Right: Deactivation of solid phase (particle ‘2’).

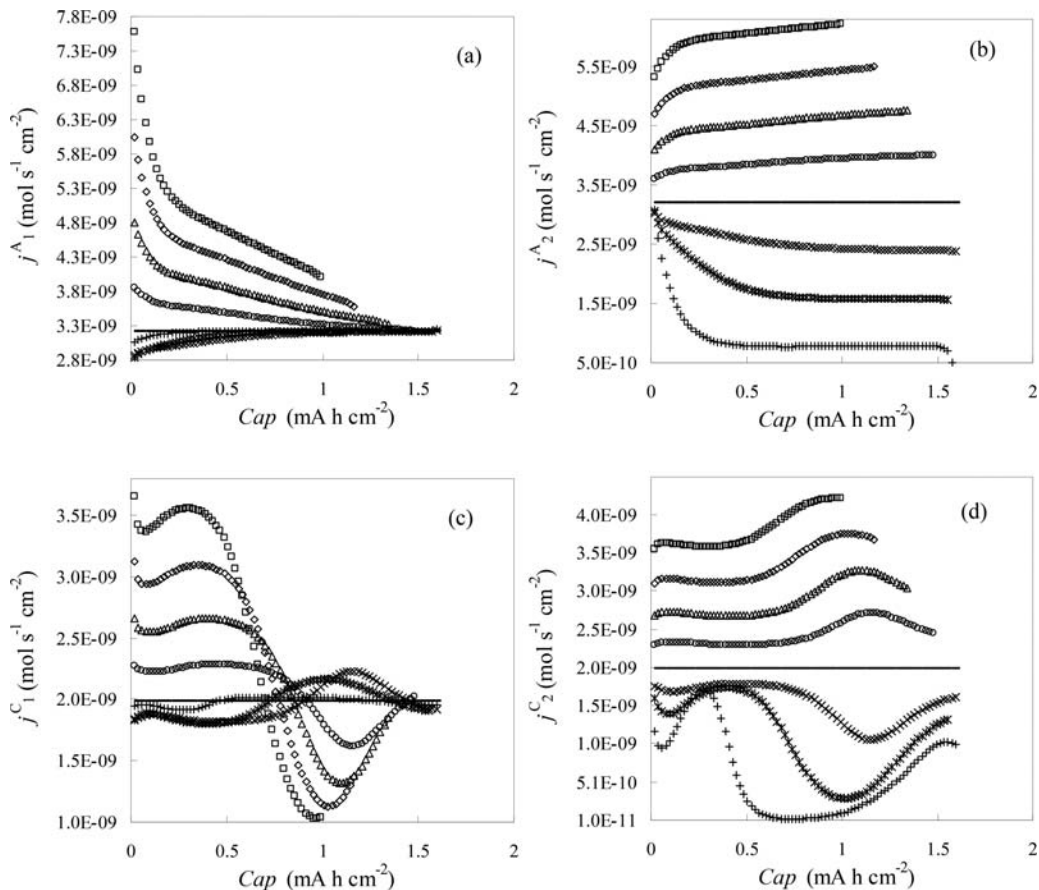


Figure 3. Evolution of reaction rates at constant discharge current, considering two particle sizes. $i_{app} = 0.0035 \text{ Acm}^{-2}$.

(a) Particle 1 in anode. (b) Particle 2 in anode. (c) Particle 1 in cathode. (d) Particle 2 in cathode. Square: $R_{s,2}/R_{s,1} = 2.00$. Rhombus: $R_{s,2}/R_{s,1} = 1.75$. Triangle: $R_{s,2}/R_{s,1} = 1.50$. Circle: $R_{s,2}/R_{s,1} = 1.25$. Line: $R_{s,2}/R_{s,1} = 1.00$. Cross: $R_{s,2}/R_{s,1} = 0.75$. Star: $R_{s,2}/R_{s,1} = 0.50$. Plus sign: $R_{s,2}/R_{s,1} = 0.25$.

411 **Cell voltage**

412 Cell voltage was calculated at a representative constant dis-
 413 charge current of $0.000875 \text{ Acm}^{-2}$, until it reaches a value
 414 below 1.5 V, and considering different particle-size ratios
 415 ($R_{s,2}/R_{s,1} = 3.00; 2.00; 1.75; 1.50; 1.25; 1.00; 0.75; 0.5$). As
 416 the ratio of sizes is greater, the battery performance is nega-
 417 tively affected. For example, battery which has particle-size
 418 relation equal to 2, reduces its final capacity in nearly 10%
 419 against a battery with uniform particle sizes, which implies an
 420 approximate reduction time of 12 min, for this cell configura-
 421 tion (discharging times of a battery, considering a single parti-
 422 cle size can be corroborated in Ref. 7 Table 4). And another
 423 whose particle-size relation is equal to 3, worsens its perfor-
 424 mance by almost 27% compared to that has no size distribu-
 425 tion, which it involves 34 min less on operation. If the battery
 426 is discharged to intermediate discharge rate (0.0035 Acm^{-2})
 427 the final capacity would decrease by about 50% comparing
 428 $R_{s,2}/R_{s,1} = 2.00$ vs. $R_{s,2}/R_{s,1} = 1.00$ cases. And if the battery is
 429 discharged to the higher simulated current (0.007 Acm^{-2}), the
 430 reduction of performance, would be around 60%, analyzing
 431 the same aforementioned case.

432 **Reaction rate**

F3 433 Figure 3 shows the evolution of anodic and cathodic electro-
 434 chemical reaction rates which are parametric to the relations
 435 between particle sizes. Figures 3a, b corresponds to anodic

particles 1 and 2, respectively. Figures 3c, d corresponds to 436
 the cathodic particles. The lines that appear with no variation 437
 correspond to simulations that consider both particles of the 438
 same size. The scheme of particle-size variation is similar to 439
 that previously described. Particle size 1 remained constant 440
 and particle size 2 was varied. 441

Figure 3a shows that the higher the quotient size—greater 442
 than 1—, the higher the initial rate on particle 1 and the reaction 443
 rate over time on particle 1. Consequently, there is a 444
 greater amount of converted lithium inside particles at the 445
 initial instants; and the battery is discharged faster. When the 446
 relationship between sizes is lower than one, initial velocities 447
 become smaller and the battery capacity is increased. In the 448
 latter cases, however, it is initially observed that the trend is 449
 not as expected as there is an apparent crossing of initial reac- 450
 tion rates and reaction rates over time. In Figure 3b, the same 451
 trends can be seen. On the contrary to what happens with parti- 452
 cle 1, velocities increase over time for ratios greater than 1 453
 and decrease for ratios lower than 1. Here, it can be observed 454
 the importance of having a simplified model with phenomeno- 455
 logical significance to analyze the behavior of these variables. 456
 In the same compartment, while some particles increase their 457
 electrochemical lithium conversion rate, others decrease. It 458
 can be seen on the left-hand scale of Figures 3a, b that the 459
 reaction rates of both particles are cross linked when the bat- 460
 tery is about 25% of its discharge, considering the largest dis- 461
 persion between the sizes. 462

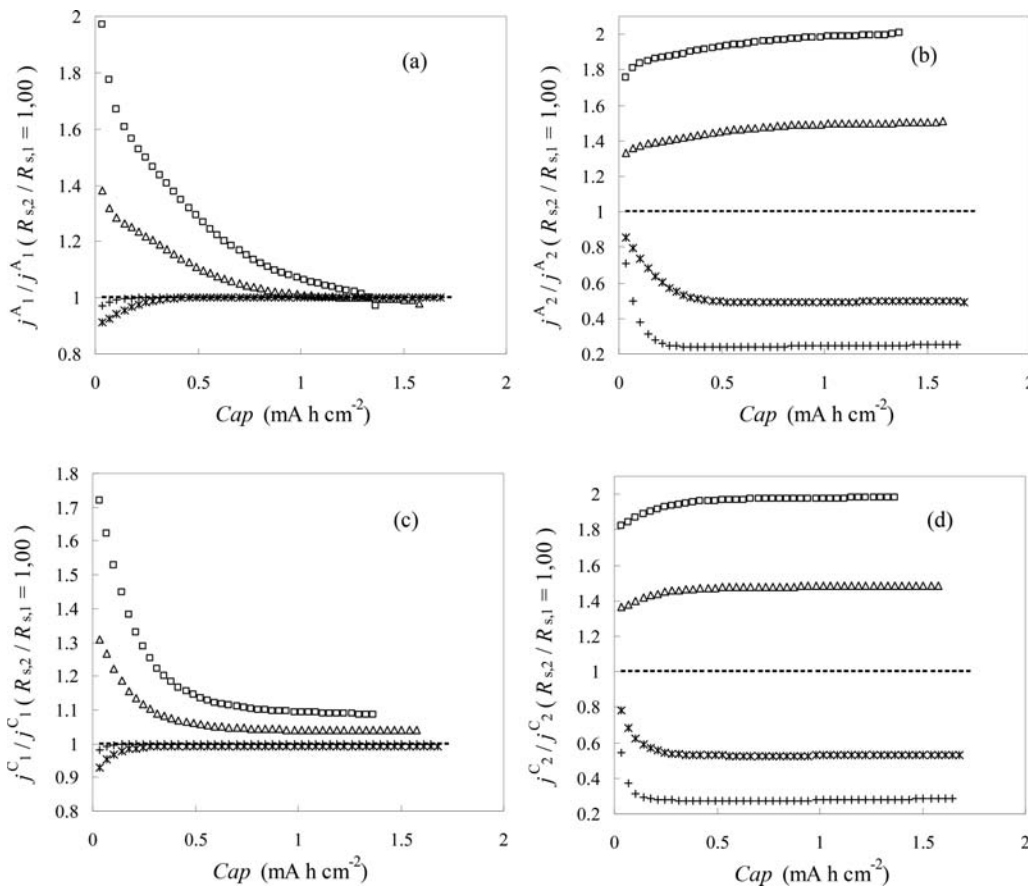


Figure 4. Evolution of reaction rates at constant discharge current, considering Eq. 35. $i_{app} = 0.00175 \text{ Acm}^{-2}$.

(a) Particle 1 in anode. (b) Particle 2 in anode. (c) Particle 1 in cathode. (d) Particle 2 in cathode. Square: $R_{s,2}/R_{s,1} = 2.00$. Triangle: $R_{s,2}/R_{s,1} = 1.50$. Line: $R_{s,2}/R_{s,1} = 1.00$. Star: $R_{s,2}/R_{s,1} = 0.50$. Plus sign: $R_{s,2}/R_{s,1} = 0.25$.

463 Reaction rates of cathodic particles are more complex to be
 464 analyzed, as, as shown in Figures 3c, d, there is a temporal
 465 evolution crossing. These crossings are due to the Plateau
 466 shape of the cathodic equilibrium potential (Eq. A2). To avoid
 467 this masking caused by the oscillations of these Plateaus, Eq.
 468 A2 is replaced by an equation arising from a logarithmic fit of
 469 these points without inflexion points

$$U_{\theta}^C = -0.153 \text{ LN}(\theta^C) + 3.955 \quad (31)$$

470 The dimensionless reaction rate for a typical value of intermedi-
 471 ate current for some values of radius ratio is shown in Figure 4.
 472 Dimensionless reaction rate refers to a cell working with par-
 473 ticles of the same size. With this modification in the U_{θ} equa-
 474 tion, cathodic behavior becomes similar to anodic one. Reaction
 475 rates for particle 1 both in cathode and anode show unexpected
 476 crossing for radius ratios lower than 1. This situation is related
 477 to the difference in external surface area of electrodes. In fact,
 478 comparisons performed up to this point involve batteries with
 479 the same active material volume and the same number of par-
 480 ticles. Analysis of batteries with the same active material vol-
 481 ume and the same electrode surface area is presented forward.

482 Capacity

483 Comparisons performed in the last section correspond to
 484 batteries with different particle sizes and the same amount of
 485 active electrode volume. A further condition was imposed by
 486 defining the number of particles “1” equal to the number of
 487 particles “2.” To assess the impact of particle-size difference,

batteries with the same electrode surface area will be compared
 instead of batteries with equal number of particles. Under this
 new frame, particle-size distribution becomes a variable. The
 problem can be defined as: Given the batteries showing the same
 dimensions and the same volume of active material and the same
 external surface area of electrodes, capacity will be computed for
 different particle sizes and, consequently, for different number of
 particles. Figures 5a, b show battery capacities discharging at
 constant current for different number of particles “1” and “2”
 which are parametric with the number of the other particle. In
 this study, radius “1” are lower than radius “2” but the number
 of particles “1” are not necessarily greater than number of par-
 ticles “2.” Figure 5a shows two different regions depending on
 the value of n_1^A . For values greater than $6e^5$, the greater the
 number of particles “2,” the higher the capacity, while for values
 lower than $6e^5$, the greater the number of particles “2,” the
 lower the final capacity. Conversely, Figure 5b depicts a differ-
 ent behavior, the higher the number of particles “1” for a given
 number of particles “2,” the lower the capacity. These tenden-
 cies can be easily explained resorting to the computation of a
 parameter defined as: difference in particle radius divided by the
 average particle radius. Figure 5c shows this parameter as func-
 tion of number of particles computed in the simulations of Fig-
 ures 5a, b. This parameter is a measure of the impact of particle-
 size distribution for batteries with the same amount of active
 material and the same electrode surface area. The greater the
 radius difference, the worse the battery performance.

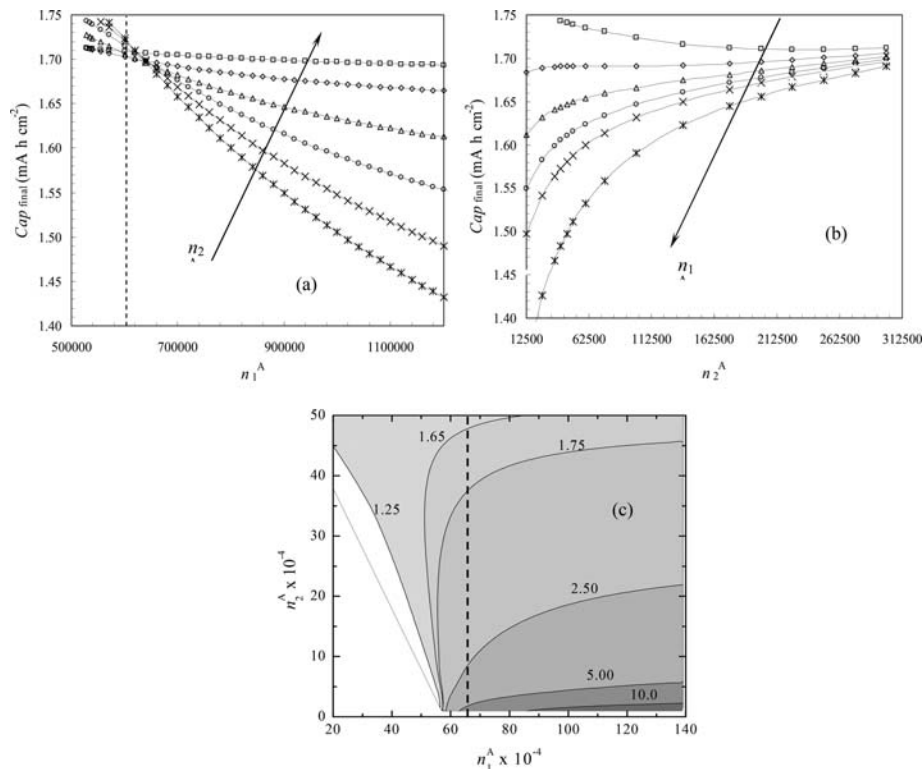


Figure 5. Battery final capacities as a function of n_1^A .

(a) the number of particle “1” with the number of particle “2” as a parameter. Square: $n_2^A = 3,00,000$. Rhombus: $n_2^A = 2,00,000$. Triangle: $n_2^A = 1,00,000$. Circle: $n_2^A = 50,000$. Cross: $n_2^A = 25,000$. Star: $n_2^A = 12,500$. (b) the number of particle “2” with the number of particle “1” as a parameter. Square: $n_1^A = 54,00,00$. Rhombus: $n_1^A = 66,00,00$. Triangle: $n_1^A = 7,80,000$. Circle: $n_1^A = 90,0000$. Cross: $n_1^A = 1,020,000$. Star: $n_1^A = 1,50,0000$. (c) Level curves of $\text{abs}(R_{s,1}^A - R_{s,2}^A) * (R_{s,1}^A + R_{s,2}^A)$. $i_{app} = 0.00175 \text{ Acm}^{-2}$.

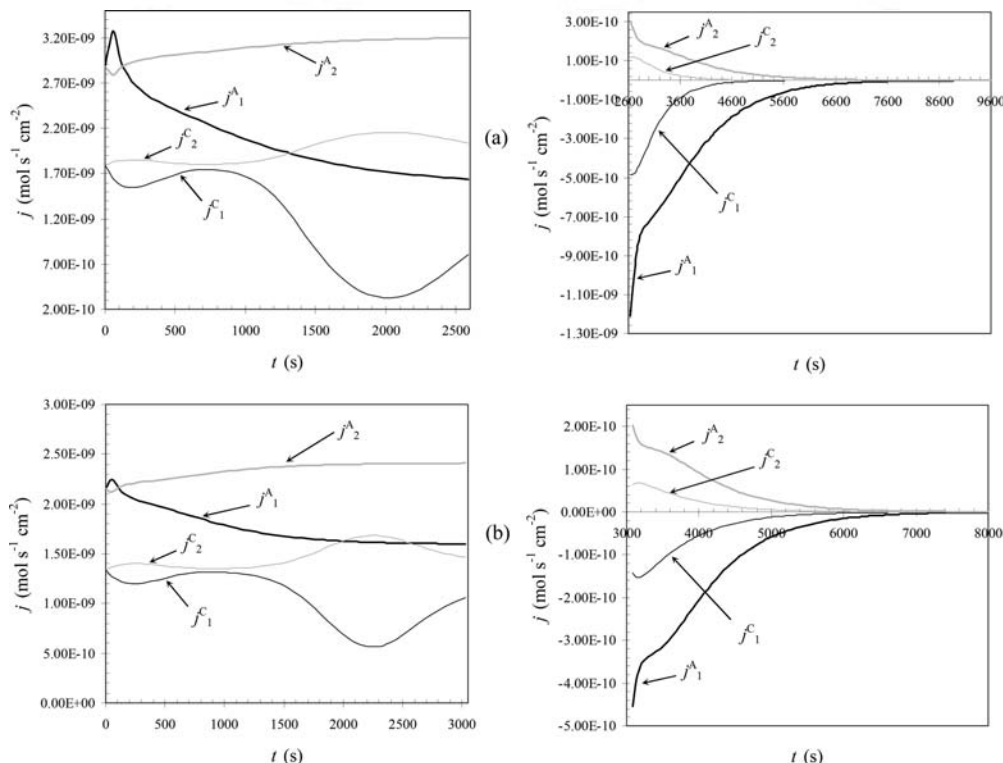


Figure 6. Reaction rate evolution at a constant discharge current and for two-size relations. Left: discharge. Right: without current. $i_{app} = 0.00175 \text{ mA cm}^{-2}$.

(a): $R_{s,2}/R_{s,1} = 2.00$. (b): $R_{s,2}/R_{s,1} = 1.50$.

516 **Results of the Model Considering Relaxation**

517 As it was discussed in Ref. 7, relaxation times in the process
 518 of discharge of a battery are very important due to the physico-
 519 chemical phenomena that influence the next batteries cycles
 520 (charges or discharges). If the electrodes of a battery have par-
 521 ticles of different sizes, it is expected that these phenomena
 522 are more radically affected.

523 To study the characteristic variables of the battery, constant
 524 current discharges up to 2.7 volts were simulated. Batteries
 525 involve particles “1” and “2” with the same amount of active
 526 material and the same number of particles “1” and “2.” Once
 527 discharge was turned off, variables involved in the simulations
 528 were computed as a time function.

529 The simulation results in cell voltage, indicate that the
 530 higher the relationship between particle radius, the lower the
 531 battery final capacity. Furthermore, voltage restitution after
 532 relaxation time is smaller when the ratio of particle size is
 533 smaller.

534 For example, for a typical low current discharge (0.000175
 535 Acm^{-2}), a battery with uniform particle size, would be dis-
 536 charged at 637 min, while a battery with $R_{s,2}/R_{s,1}=2$ is dis-
 537 charged in 622 min. Likewise relaxation times in battery with
 538 uniform particle size, would be relatively short, approximately
 539 7 min. And 48 min for the case $R_{s,2}/R_{s,1} = 2$. If the same calcu-
 540 lation is performed for a discharge current slightly higher,
 541 0.00175 Acm^{-2} , the discharge times are 3400 and 2600 s and
 542 the relaxation times are 450 and 2200 s, respectively ($R_{s,2}/$
 543 $R_{s,1} = 1$ and $R_{s,2}/R_{s,1} = 2$).

544 Once again, the importance of having a model such as the
 545 one presented in this paper is evident, to predict these phenom-
 546 ena. This model, differential in time, integral in space, allows
 547 us to evaluate this dramatic change in the total duration of the
 548 charge of the battery, being subjected to a controlled discharge
 549 at constant current. It can be inferred that if the discharge is
 550 performed under nonideal conditions (e.g., with the discharge
 551 and recharge cycles typical of an electric car) these discrepan-
 552 cies would be even greater.

553 This fact would indicate, once more, that battery perform-
 554 ance is negatively affected by particle-size distribution in
 555 the electrodes. That is, even though the batteries with higher
 556 ratios between particle sizes reach a relative higher voltage at
 557 the relaxation stage, their delivered capacity was lower and
 558 they took longer to reach the new equilibrium state.

559 Figure 6 depicts the evolution of reaction rates for an inter-
 560 mediate current and for two values of particle-size relation-
 561 ships before and after the discharge of the battery. Discharge
 562 periods were analyzed in previous sections. At relaxation
 563 moments, an abrupt reduction of current densities takes place
 564 (note differences in the graph scales). Anode particles take
 565 longer to reach the equilibrium; and this phenomenon is more
 566 evident for the battery of Figure 6a, where in the dispersion
 567 among particle sizes of electrodes is the greatest, again indi-
 568 cating the negative contribution of this size difference.

F7 569 Finally, Figure 7 shows, the values taken by the overpoten-
 570 tial of the different particles of both electrodes, Figure 7a, and
 571 conversely, the difference in equilibrium potentials of both
 572 electrodes, Figure 7b. This analysis is performed for a typical
 573 current value and a typical size distribution value.

574 Figure 7 also depicts the behavior of the continuity of the
 575 electric field Eq. 29 both in discharge zone and relaxation
 576 zone. The abrupt jump in the values of variables is detected
 577 around 3000 s after discharge. Again, it becomes evident that
 578 relaxation of anode particles (thicker lines, Figure 7a) takes

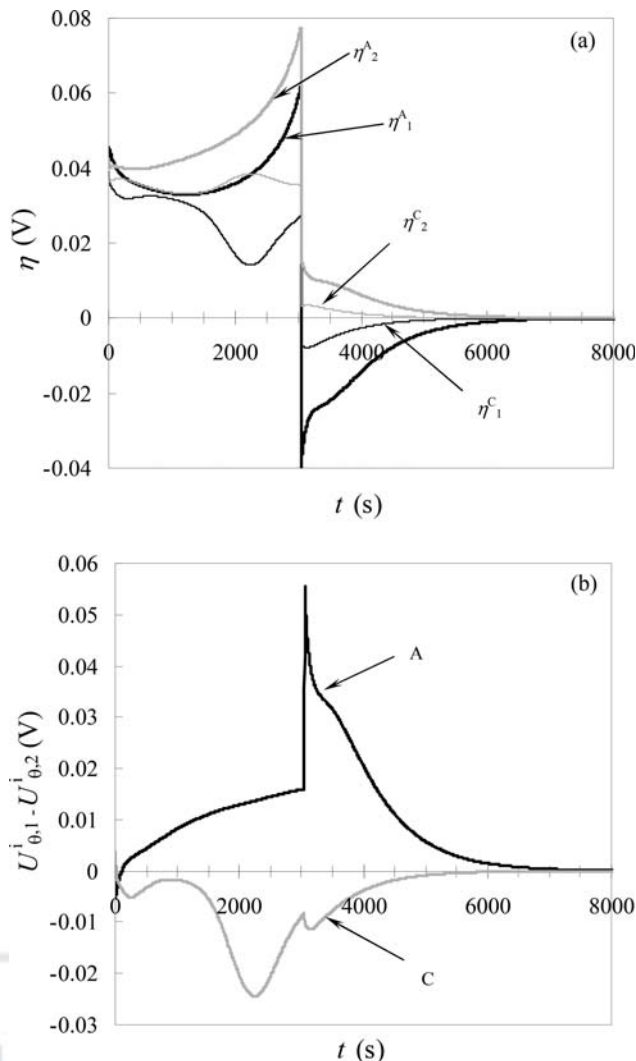


Figure 7. Continuity of electric field.
 (a) overpotentials. (b) difference in equilibrium potentials $i_{app}: 0.00175 \text{ mA cm}^{-2}$. $R_{s,2}/R_{s,1} = 1.50$. AQ8

longer than that of cathode particles. This effect can be
 explained by taking into account the different shapes of equi-
 librium potentials, U_{θ} , and the fact that anode particles are
 larger than cathode particles in these batteries. So, finally,
 there is evidence to account not only for the size of particles
 themselves, but also for the distribution of particle sizes in
 electrodes.

The negative influence of particle-size distribution on the
 electrodes of a lithium-ion battery has been demonstrated,
 which is the attained objective of this study.

Furthermore, evidence has been provided for the importance
 of addressing these factors in battery manufacturing.

Conclusions

1. The performance of lithium ion was studied by solving a novel mathematical model in two different scenarios: (i) maintaining constant the amount of active electrode material and varying the particle size, (ii) maintaining constant volume and the electrode surface area and varying the number of each of the particles.

598 2. This model has been validated by experimental points
 599 provided by other authors and using two different types
 600 of cells.
 601 3. With this simplified model, large discrepancies in the final
 602 duration of a battery considering different particle sizes
 603 and batteries with a homogeneous particles sizes were
 604 found. This feature is much appreciated for predicting the
 605 behavior of batteries in large facilities.
 606 4. Some comparisons between the model and the experimen-
 607 tal points were significantly improved by varying the par-
 608 ticle sizes of the electrodes.
 609 5. Plateaus existence in the cathode equilibrium potential
 610 impacts markedly in the current density distribution
 611 between particles of different sizes.
 612 6. Differences between particles sizes of the electrodes, neg-
 613 atively affects the performance of the battery. At high dis-
 614 charge current, difference between the particle sizes of
 615 50%, reduces up to 35% battery capacity.
 616 7. By maintaining constant the number of one particle type,
 617 significant variations in battery capacity are obtained by
 618 varying the number of the other particle, keeping constant
 619 the total amount of material.
 620 8. Relaxation times of a partially discharged battery are also
 621 affected by the fact of having particles with different
 622 sizes. Relaxation occurs 25% faster on batteries with uni-
 623 form particle size, comparing them against batteries that
 624 have a dispersion size of 100%.

625 Acknowledgments

626 The authors acknowledge financial support provided by
 627 Consejo Nacional de Investigaciones Científicas y Técnicas
 628 (CONICET), Agencia Nacional de Promoción Científica y
 629 Tecnológica (ANPCyT) of Argentina, and Facultad de
 630 Ingeniería Química, Universidad Nacional del Litoral
 631 (UNL).

632 Notation

636 a = area, cm^2
 639 Cap = capacity, mA h cm^{-2}
 640 C = concentration, mol cm^{-3}
 643 i = current density, mA cm^{-2}
 648 D = diffusion coefficient, $\text{cm}^2 \text{s}^{-1}$
 650 F = Faraday's constant: $96485.34, \text{C mol}^{-1}$
 653 j = electrochemical reaction rate, $\text{mol s}^{-1} \text{cm}^{-2}$
 655 j_0 = exchange current density, mA cm^{-2}
 660 K = constants in Eq. 15
 662 K_1^{\pm} = mass transfer coefficient between anode ($i = A$) and separator
 664 and separator and cathode ($i = C$), cm s^{-1}
 665 k = constant rate of the electrochemical reaction
 668 k_i ($i = 1; 2; 3; 4$) = constants in Eqs. 31–33
 671 L = electrode length, cm
 675 n = number of solid particles
 679 ntp = transport number
 680 N = usage cycle
 683 U = potential, V
 688 R_g = universal gas constant $8.314, \text{J mol}^{-1} \text{K}^{-1}$
 690 R_p^0 = resistance between particles, Eq. 34
 693 $R_{s,m}^i$ = solid particle radius of the particle “m” on the electrode “i”, cm
 695 t = time, s
 698 T = temperature, K
 701 v = volume, cm^3

704 Specials and Greek letters

708 t_+^0 = transport number
 709 f_{\pm} = molar activity coefficient of the salt
 713 ε = volume fraction
 715 δ = diffusion distance, cm

κ = electrolyte conductivity, S cm^{-1} 719
 $\Delta\phi$ = potential drop, V 721
 σ = solid conductivity, S cm^{-1} 725
 θ = state of charge 729
 η = overpotential, V 730
 fraction = fraction of the current drained by particles 735

Subscript

app = applied 736
 e = electrolyte 739
 eff = effective 741
 e/s = electrolyte in contact with solid 746
 n, m = particle number 749
 s = solid 750
 f = filler 753
 p = polymer 758
 l = liquid 760
 tr.e = transversal area of electrolyte phase 763
 tr.s = transversal area of solid phase 766
 t = transversal 771
 o = pure 776
 θ = open circuit potential 779
 cell = cell 780
 diff = diffusion 783
 int = interior 788
 ext = exterior 790
 max = maximum 793
 surf = surface 796

Superscript

i = anode, cathode or separator 798
 A = anode 800
 C = cathode 803
 S = separator 806
 γ = Bruggeman's exponent 809
 0 = initial 813
 o = pure 815

Literature Cited

1. Tarascon JM, Armand M. Issues and challenges facing rechargeable
 822 lithium batteries. *Nature*. 2001;414:359–367. 823
 2. Owen JR. Rechargeable lithium batteries. *Chem Soc Rev*. 1997;26:
 824 259–267. 825
 3. Doyle M, Newman J, Gozdz AS, Schmutz CN, Tarascon JM. Com-
 826 parison of modelling predictions with experimental data from plastic
 827 lithium ion cell. *J Electrochem Soc*. 1996;143(6):1890–1903. 828
 4. Santhanagopalan S, Guo Q, Ramadass P, White RE. Review of mod-
 829 els for predicting the cycling performance of lithium ion batteries.
 830 *J Power Sources*. 2006;156:620–628. 831
 5. Erdinc O, Vural B, Uzunoglu M. A dynamic lithium-ion battery
 832 model considering the effects of temperature and capacity fading. In:
 833 *IEEE 2009 International Conference on Clean Electrical Power*.
 834 Capri, Italy, 9–11 June 2009:383–386. 835
 6. Shen J-N, He Y-J, Ma Z-F. Simultaneous model selection and
 836 parameter estimation for lithium-ion batteries: a sequential MINLP
 837 solution approach. *AIChE J*. 2016;62(1):78–89. 838
 7. Henquín ER, Aguirre PA. Phenomenological model-based analysis
 839 of lithium batteries: discharge, charge, relaxation times studies, and
 840 cycles analysis. *AIChE J*. 2015;61(1):90–102. 841
 8. Ramadass P, Haran B, White R, Popov BN. Mathematical modeling
 842 of the capacity fade of Li-ion cells. *J Power Sources*. 2003;123:230–
 843 240. 844
 9. Zhang D, Popov BN, White RE. Modeling lithium intercalation of a
 845 single spinel particle under potentiodynamic control. *J Electrochem*
 846 *Soc*. 2000;147(3):831–838. 847
 10. Doyle M, Fuller TF, Newman J. Modeling of Galvanostatic charge
 848 and discharge of the lithium/polymer/insertion cell. *J Electrochem*
 849 *Soc*. 1993;140:6. 850
 11. Ramadesigan V, Northrop PWC, De S, Santhanagopalan S, Braatz
 851 RD, Subramaniana VR. Modeling and simulation of lithium-ion bat-
 852 teries from a systems engineering perspective. *J Electrochem Soc*.
 853 2012;159(3):R31–R45. 854
 12. Chung D-W, Shearing PR, Brandon NP, Harris SJ, Edwin García R.
 855 Particle size polydispersity in Li-ion batteries. *J Electrochem Soc*.
 856 2014;161(3):A422–A430. 857

- 858 13. Zaghbi K, Brochu F, Guerfi A, Kinoshita K. Effect of particle size
859 on lithium intercalation rates in natural graphite. *J Power Sources*.
860 2001;103:140–146.
- 861 14. Sheu SP, Yao CY, Chen JM, Chiou YC. Influence of the LiCoO₂
862 particle size on the performance of lithium-ion batteries. *J Power*
863 *Sources*. 1997;68:533–535.
- 864 15. Lu C-H, Lin S-W. Influence of particle size on the electrochemical
865 properties of lithium manganese oxide. *J Power Sources*. 2001;97–
866 98:458–460.
- 867 16. Vacassy R, Hofmann H, Papageorgiou N, Grätzel M. Influence of
868 the particle size of electrode materials on intercalation rate and
869 capacity of new electrodes. *J Power Sources*. 1999;81–82:621–626.
- 870 17. Liu J, Wang Z, Zhang G, Liu Y, Yu A. Size-controlled synthesis of
871 LiFePO₄/C composites as cathode materials for lithium ion batteries.
872 *Int J Electrochem Sci*. 2013;8:2378–2387.
- 873 18. Smith M, Garcia RE, Hornb QC. The effect of microstructure on the
874 Galvanostatic discharge of graphite anode electrodes in LiCoO₂-
875 based rocking-chair rechargeable batteries. *J Electrochem Soc*. 2009;
876 156(11):A896–A904.
- 877 19. Doherty CM, Caruso RA, Drummonda CJ. High performance
878 LiFePO₄ electrode materials: influence of colloidal particle morphol-
879 ogy and porosity on lithium-ion battery power capability. *Energy*
880 *Environ Sci*. 2010;3:813–823.
- 881 20. Kai K, Kobayashi Y, Miyashiro H, Oyama G, Nishimura S-I, Okubo
882 M, Yamada A. Particle-size effects on the entropy behavior of a Li_x-
883 FePO₄ electrode. *Chemphyschem*. 2014;15(10):2156–2161.
- 884 21. Utsunomiya T, Hatozaki O, Yoshimoto N, Egashira M, Morita M.
885 Influence of particle size on the self-discharge behavior of graphite elec-
886 trodes in lithium-ion batteries. *J Power Sources*. 2011;196:8675–8682.
22. Qi X, Blizanac B, DuPasquier A, Oljaca M, Li J, Winter M. Under- 887
888 standing the influence of conductive carbon additives surface area on
889 the rate performance of LiFePO₄ cathodes for lithium ion batteries.
890 *Carbon*. 2013;64:334–340.
23. Ren Y, Armstrong AR, Jiao F, Bruce PG. Influence of size on the 891
892 rate of mesoporous electrodes for lithium batteries. *J Am Chem Soc*.
893 2010;132:996–1004.
24. Stephenson DE, Hartman EM, Harb JN, Wheeler DR. Modeling of 894
895 particle-particle interactions in porous cathodes for lithium-ion bat-
896 teries. *J Electrochem Soc*. 2007;154(12):A1146–A1155.
25. Du W, Gupta A, Zhang X, Sastry AM, Shyy W. Effect of cycling 897
898 rate, particle size and transport properties on lithium-ion cathode
899 performance. *Int J Heat Mass Transf*. 2010;53:3552–3561.
26. Kenney B, Darcovich K, MacNeil DD, Davidson IJ. Modelling the 900
901 impact of variations in electrode manufacturing on lithium-ion bat-
902 tery modules. *J Power Sources*. 2012;213:391–401.
27. Darling R, Newman J. Modeling a porous intercalation electrode with two 903
904 characteristic particle sizes. *J Electrochem Soc*. 1997;144:4201–4208.
28. Srinivasan V, Newman J. Discharge model for the lithium iron- 905
906 phosphate electrode. *J Electrochem Soc*. 2004;151(10):A1517–A1529.
29. Thorat IV, Joshi T, Zaghbi K, Harb JN, Wheeler DR. Understanding 907
908 rate-limiting mechanisms in LiFePO₄ cathodes for Li-Ion batteries.
909 *J Electrochem Soc*. 2011;158(11):A1185–A1193.
30. Brooke A, Kendrick D, Meeraus A, Raman R. GAMS Language 910
911 Guide, RELEASE 2.25, Version 92. Washington, DC:GAMS Devel-
912 opment Corporation, 1997.
31. Available at: <http://www.scilab.org/> (Accessed 10, October, 2017). 913
- 914
915

Manuscript received Oct. 12, 2016, and revision received Apr. 20, 2017.

916

WILEY
Author Proof